Antiferromagnetism and the Magnetic Phase Diagram of $GdAlO_3$

K. W. Blazey and H. Rohrer
IBM Zurich Research Laboratory, 8803 Rüschlikon-ZH, Switzerland

(Received 15 February 1968; revised manuscript received 24 May 1968)

Measurements of the magnetization and differential susceptibility of $GdAlO_3$ have been made in pulsed magnetic fields in the temperature range 1.3–100°K. It is found that $GdAlO_3$ is a uniaxial antiferromagnet with the easy axis of magnetization along the orthorhombic b axis. The Néel temperature is found to be 3.89°K and the Curie-Weiss $\Theta = -4.6$°K. The gradient of the inverse molar susceptibility shows the ionic moment of Gd to be 7 μ_B, but this full moment is never observed in the high-field magnetization, even in fields of 200 kOe at 1.3°K. The differential susceptibility has been used to observe both the antiferromagnetic-to-spin-flop and the spin-flop-to-paramagnetic phase transitions, and to determine the phase diagram in the H-T plane. The molecular-field parameters have been calculated from the antiferromagnetic-to-spin-flop transition and the angular variation of the spin-flop-to-paramagnetic transition.

INTRODUCTION

CONSIDERABLE attention has recently been given to the magnetic phase transitions of uniaxial antiferromagnets and the resultant phase diagram in the H-T plane.[1,2] The number of uniaxial antiferromagnets with a combination of readily attainable exchange fields, Néel temperature, and easy growth of chemically stable single crystals is, however, rather limited. Here we report the magnetic properties of such a material, the perovskite $GdAlO_3$.

Magnetic materials with the perovskite structure ABO_3 have been extensively studied in the past.[3] These studies, however, have been made primarily on compounds with either transition-metal ions on the B site as the only magnetic ion present, or a combination of transition-metal ions on the B site and rare-earth ions on the A site. Only recently have studies of the magnetic properties of perovskites containing only rare earths as the magnetic ion been initiated.

The x-ray analysis of $GdAlO_3$ and a wide range of analogous materials has been reported by Geller and Bala.[4] They found that $GdAlO_3$ is orthorhombic, isostructural with $GdFeO_3$, and belongs to the space group D_{2h}^{16}-$Pbnm$ with four distorted perovskite units in the crystallographic unit cell. It has previously been reported that $GdAlO_3$ shows a transition to antiferromagnetism at low temperatures.[5] Here we wish to report its magnetic properties in more detail.

The susceptibility, magnetization, and differential susceptibility have been measured in pulsed magnetic fields up to 200 kOe in the temperature range 1.3–100°K. It is found that $GdAlO_3$ is a uniaxial antiferromagnet with a Néel temperature of 3.89°K and that the highest field-induced phase transition occurs at 42.0 kOe at 0°K. These two properties, plus the fact that single crystals are readily grown, make $GdAlO_3$ an attractive material for an experimental study of antiferromagnetism.

The magnetic phase transitions can be observed in both the magnetization and the differential susceptibility. At the antiferromagnetic-to-spin-flop first-order phase transition, where the spins change their alignment from parallel to perpendicular to the easy axis of magnetization, the magnetization shows a discontinuity and the differential susceptibility a sharp peak. The spin-flop-to-paramagnetic transition, where the angle between the two sublattice magnetizations goes to zero, is a second-order phase transition. In this case only the differential susceptibility gives a satisfactory and accurate location of the transition.

The basic measurements of the pulsed-field technique are the time derivatives of the magnetic field dH/dt and the magnetization dM/dt. Division of these two signals gives directly the differential susceptibility dM/dH. Thus the critical fields for these transitions were determined as a function of temperature and the phase diagram in the H-T plane determined. The determination of the critical fields from the differential susceptibility has the added advantage that the detailed form of the transition itself may be determined, but this will be reported in another paper.

EXPERIMENTAL

Measurements were made on both sintered powders and flux-grown crystals. The starting materials in both cases were Gd_2O_3 of purity better than 99.9% and Al_2O_3 of 99.998% purity obtained from Fluka Chemicals. The powders were sintered three times at 1400°C after being ball-milled and compressed into pellet form. The single crystals were grown in this laboratory by R. Webster using a PbO–PbF_2 flux method as reported by Linares.[6] Clear rectangular-shaped crystals were obtained with side lengths varying up to 4 mm.

The magnetization and differential susceptibility measurements were carried out on spheres ground

[1] F. B. Anderson and H. B. Callen, Phys. Rev. **136**, 1068 (1964).
[2] J. Feder and E. Pytte, Phys. Rev. **168**, 640 (1968).
[3] J. S. Smart, in *Magnetism*, edited by G. T. Rado and H. Suhl (Academic Press Inc., New York, 1963), Vol. 3.
[4] S. Geller and B. Bala, Acta Cryst. **9**, 1019 (1956).
[5] K. W. Blazey and H. Rohrer, Helv. Phys. Acta **40**, 370 (1967).
[6] R. C. Linares, J. Appl. Phys. **33**, 1747 (1962).

from the single crystals by the method described by Bond.[7]

The pulsed-field apparatus used is essentially the same as that described by Olsen and Cotti[8] where a high magnetic field is generated by the rapid discharge of a capacitor bank through a field coil immersed in liquid helium. Inside the field coil are located three smaller pickup coils. One coil contains the sample, the second is used to compensate the sample coil without sample, and the third to measure the magnetic field. The signal generated in the field measuring coil is proportional to dH/dt and may thus be integrated to yield the value of the magnetic field. Calibration of the field was carried out with the calculated coil factors.[8] The signal generated by the other two coils is proportional to the time derivative of the sample magnetization, which is integrated to give the sample magnetization. The magnetization measurement was calibrated against pure iron.

The signals dM/dt and dH/dt were also fed into an analog function generator which gave an output of dM/dH. This signal, the differential susceptibility, was used to observe the magnetic phase transitions of $GdAlO_3$.

RESULTS

1. Susceptibility

The susceptibility was measured at various temperatures in the range 1.3–100°K and at room temperature. Figure 1 shows the inverse molar susceptibility plotted against the absolute temperature. Above 4°K the inverse molar susceptibility increases virtually linearly and is independent of crystal orientation. This linear part of the graph follows a Curie-Weiss law with a molar Curie constant $C_M = 7.99 \pm 0.16$ cm³ °K/mole which should be compared with the theoretical value of 7.89 cm³ °K/mole assuming a spin of $\frac{7}{2}$ for the Gd ions. Extrapolation of this graph gives a Curie-Weiss $\Theta = -4.6$ °K.

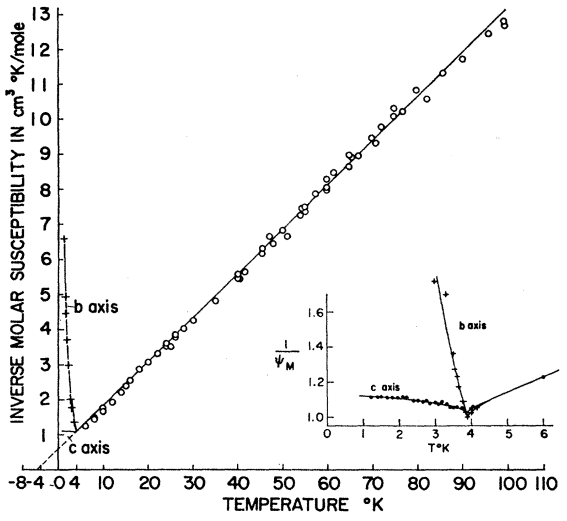

FIG. 1. Inverse molar susceptibility of $GdAlO_3$ plotted against absolute temperature.

The inverse susceptibility shows a minimum at (3.90 ± 0.02)°K, typical of a transition to an ordered antiferromagnetic state. This is 0.23°K higher than reported by Cashion *et al.*[9] Below this temperature it is seen that the inverse susceptibility for the field parallel to the orthorhombic c axis varies very little with temperature, whereas that when the field is parallel to the b axis rises steeply. This indicates that the b axis is the easy axis of magnetization. The value of the susceptibility at the Néel temperature is 0.939 ± 0.02 cm³/mole.

2. Magnetization

The magnetization of the $GdAlO_3$ spheres was measured as a function of crystal orientation in fields up to 200 kOe. For applied fields outside the spin-flop-to-paramagnetic phase transition boundary the magnetization is practically independent of crystal orientation, whereas inside this boundary the behavior is strongly orientation-dependent. Figure 2 shows the low-field magnetization along the [010] direction, the easy axis of magnetization for temperatures between 1.44 and 4.16°K. The field axis is the applied field minus the demagnetizing field of the $GdAlO_3$ sphere. The low-field magnetization shows a discontinuity at about 11 kOe typical of an antiferromagnetic-to-spin-flop transition as observed by Jacobs[10] in MnF_2. The size and sharpness of this discontinuity descreases rapidly with deviation from the [010] direction and disappears completely in directions perpendicular to the easy axis of magnetization, as shown in Fig. 3 for the $[\sqrt{2}, 0, 1]$ direction.[11] Above 11 kOe the magnetization increases linearly with applied field for all directions. In this region, the magnetization is independent of temperature and only weakly dependent on the crystal orientation. At a certain field, the magnetization breaks off from this line of linear field dependence and bends over to a region of weak field dependence. This breakoff field gives the spin-flop-to-paramagnetic critical field H_{c2}.

Outside the spin-flop-to-paramagnetic boundary, at 4.16°K and below, there is only little field dependence of the magnetization, and the full moment of $7\mu_B$ per Gd atom is never observed even at 1.3°K. This

[7] W. L. Bond, Rev. Sci. Instr. **25**, 401 (1954).
[8] J. L. Olsen, Helv. Phys. Acta **26**, 798 (1953); P. Cotti, Z. Angew. Math. Phys. **11**, 17 (1960).
[9] J. D. Cashion, A. H. Cooke, J. F. B. Hawkes, M. J. M. Leask, T. L. Thorp, and M. R. Wells, J. Appl. Phys. **39**, 1360 (1968).
[10] I. S. Jacobs, J. Appl. Phys. **32**, 61S (1961).
[11] The $[\sqrt{2}, 0, 1]$ direction in the orthorhombic cell corresponds to the $[1\bar{1}1]$ direction in the cubic pseudocell.

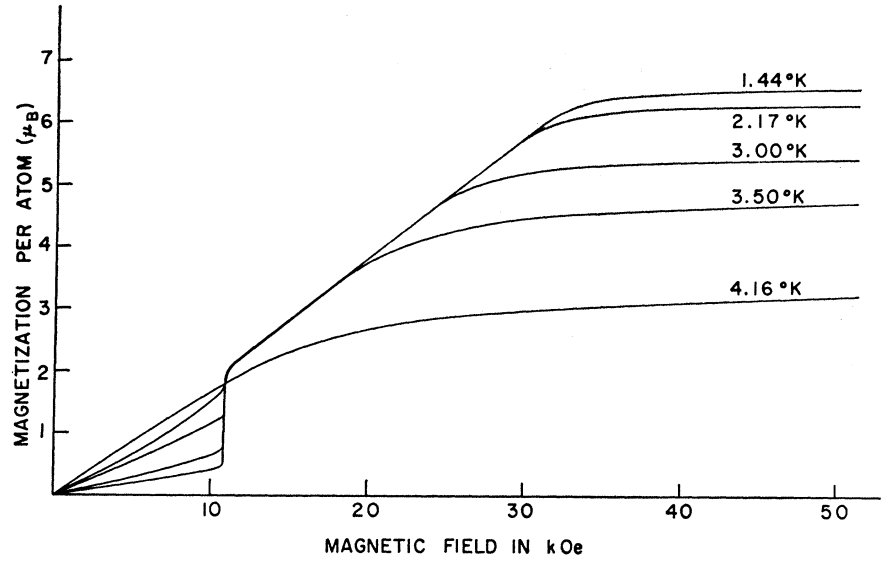

FIG. 2. Magnetization, in Bohr magnetons per atom, plotted against magnetic field applied along the orthorhombic b axis. The magnetization discontinuity at 11 kOe corresponds to the antiferromagnetic-to-spin-flop phase transition.

is entirely unexpected since for $\mu(H-H_{ex}\sigma)/kT\gg1$, where σ is the normalized magnetization[12] and H_{ex} is the exchange field defined in the discussion, all the spins should be aligned. At 190 kOe and 4.16°K, $\mu(H-H_{ex}\sigma)/kT\sim20$, and therefore the full moment is expected already at 4.16°K, whereas only $\frac{2}{3}$ of the Gd moment is observed. However, a plot of this experimentally observed plateau magnetization against temperature extrapolates to $7\mu_B$ at 0°K. Above 4.16°K the low-field magnetization behaves as expected, as is also seen in the linear form of the susceptibility graph. However, in higher field, above 50 kOe at 40°K the measured magnetization is smaller than expected. This is shown in Fig. 3, where the calculated magnetization (neglecting anisotropy) is drawn for $T=40$°K. This anomalous behavior of the magnetization in the paramagnetic region is not understood.

3. Differential Susceptibility and Magnetic Phase Diagram

At temperatures below the Néel point and in low fields the sublattice magnetizations of a uniaxial antiferromagnet are held in opposite directions along the easy axis of magnetization by the anisotropy field.

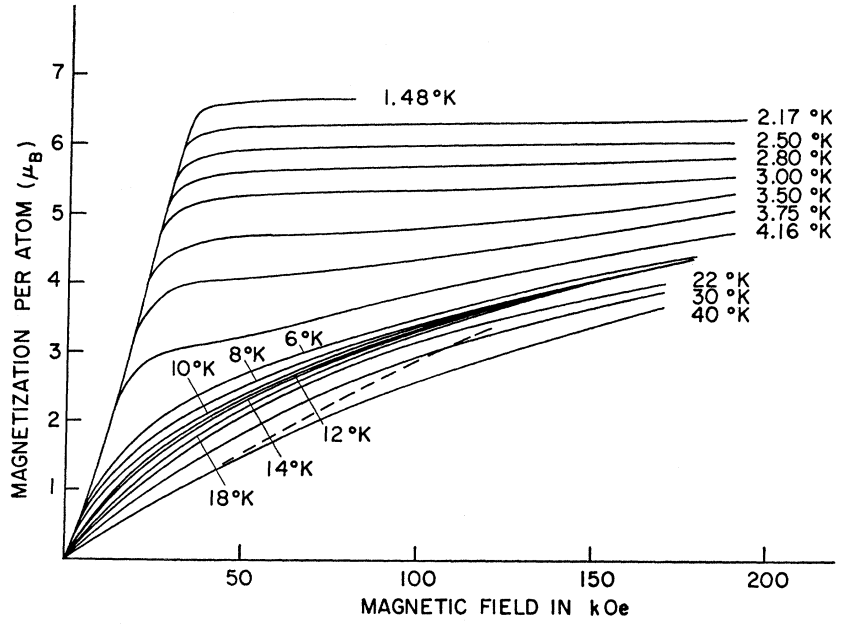

FIG. 3. Magnetization, in Bohr magnetons per atom, plotted against magnetic field applied in the $[\sqrt{2}, 0, 1]$ direction. The broken line gives the calculated magnetization for $T=40$°K.

[12] J. S. Smart, *Effective Field Theories of Magnetism* (W. B. Saunders, Philadelphia, 1966).

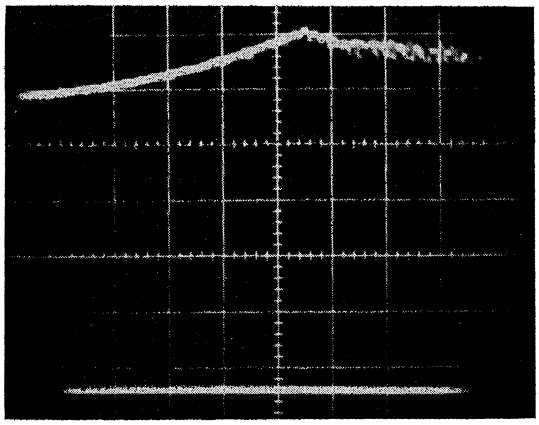

(a) $T=3.80°K$, field scale = 1050 Oe per scale division.

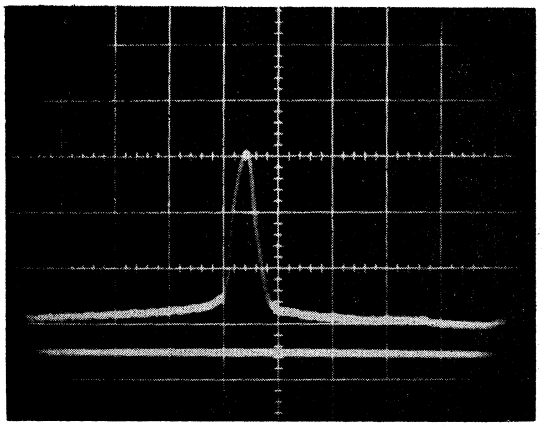

(b) $T=3.50°K$, field scale = 340 Oe per scale division.

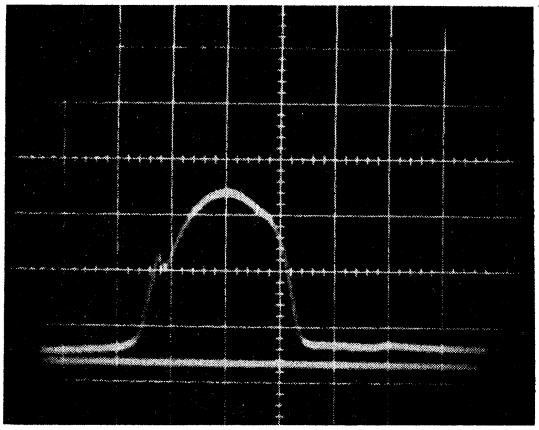

(c) $T=2.50°K$, field scale = 340 Oe per scale division.

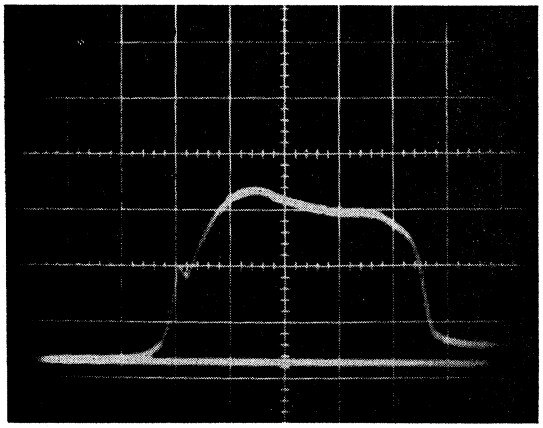

(d) $T=1.25°K$, field scale = 310 Oe per scale division.

FIG. 4. Oscillograms of dM/dH against applied magnetic field showing the growth of the peak due to spin flopping at H_{c1} as a function of temperature. The relative sensitivities (in arbitrary units) of the dM/dH scale are 20:2:1:1 for 3.80, 3.50, 2.50, and 1.25°K, respectively.

When a field parallel to this easy axis of magnetization is increased, the Zeeman energy of the spins increases less rapidly than if the spins were perpendicular to the applied field. This is simply because the perpendicular susceptibility is generally larger than the parallel susceptibility. There exists, therefore, a critical field where the energy is lower if the spins flop perpendicular to the applied field. This transition occurs when the combined anisotropy and Zeeman energies of the spins, when they are parallel to the applied fields, become less than the Zeeman energy of the spins if they were perpendicular to the applied field. Associated with this first-order phase transition there is a discontinuous jump in the magnetization as shown in Fig. 2. Differentiation of this magnetization curve would give a peak at the critical field H_{c1}. This is clearly observed in the measurement of dM/dH as a function of applied field as shown in Fig. 4. As the temperature is reduced below the Néel temperature the peak is seen to grow quickly to a certain magnitude at around 3°K and remain at this intensity down to the lowest temperature measured. Below 3°K the width and magnitude of the peak are determined by the demagnetizing field that comes with the increase in the discontinuity of the magnetization.

The width of this transition is critically dependent upon the crystal orientation.[13] For the photographs shown in Fig. 4, the crystal was aligned to better than 0.2°. At high temperatures, where the change in magnetization is small, the middle of the peak was taken as the transition field. At low temperatures, where the change in magnetization determines the observed peak width, both the fields at the beginning and end of the peak are measured. These values are then corrected for demagnetizing fields and their mean value taken as the critical field. The width of the transition so determined is of the order 200–300 Oe.

[13] S. Foner, in *Magnetism*, edited by G. T. Rado and H. Suhl (Academic Press Inc., New York, 1963), Vol. 1, p. 389.

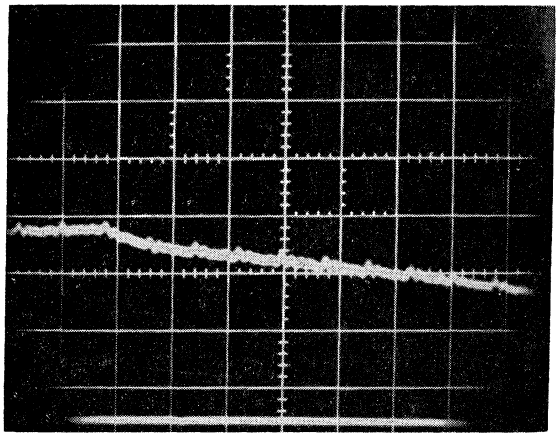

(a) $T=3.50$°K, field scale=430 Oe per scale division.

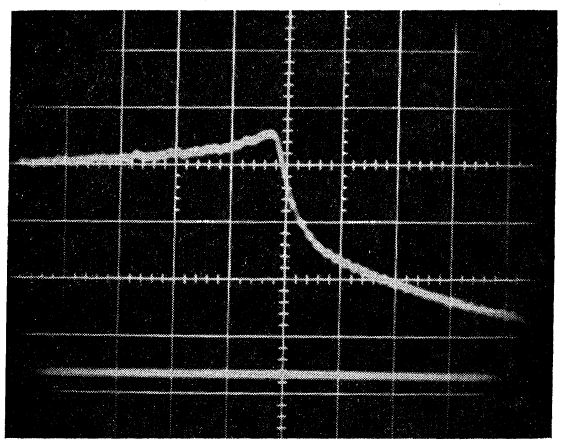

(b) $T=2.50$°K, field scale=600 Oe per scale division.

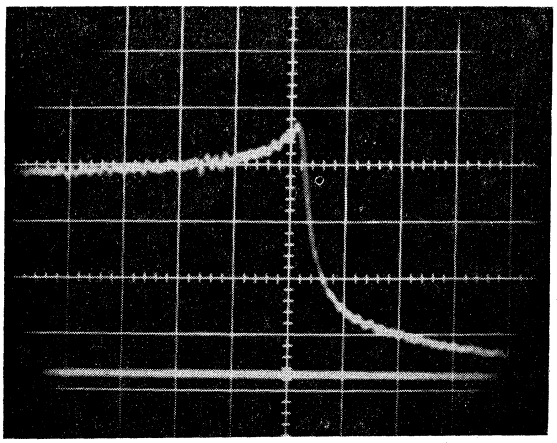

(c) $T=1.25$°K, field scale=680 Oe per scale division.

FIG. 5. Oscillograms of dM/dH against applied magnetic field showing the sharp drop in dM/dH on passing through the spin-flop-to-paramagnetic phase boundary at H_{c2}. The sensitivity of dM/dH is the same in all three photographs.

Thus the variation of the critical field H_{c1} was determined between 1.20 and 3.87°K for the applied field along the b axis.

At low temperatures, then, dM/dH is small until a field H_{c1} is reached where a peak is observed. Above this field dM/dH has a constant value close to that of the perpendicular susceptibility. This region of constant susceptibility is followed by a precipitous drop of dM/dH at low temperatures as shown in Fig. 5. This locates the spin-flop-to-paramagnetic transition, which, as a second-order phase transition should show such a discontinuity of the differential susceptibility. At temperatures close to the Néel temperature the transition is smeared out by the thermal fluctuations, but an accurate determination of the transition field H_{c2} is still possible. At still higher fields the differential susceptibility decreases rapidly, corresponding to the observed bendover in the high-field magnetization mentioned in the previous section.

The temperature variation of this critical field, H_{c2}, has been measured also from 1.2–3.8°K and is shown in Fig. 6 along with the temperature variation of H_{c1}.

The extrapolation to 0°K of the H_{c2} variation was

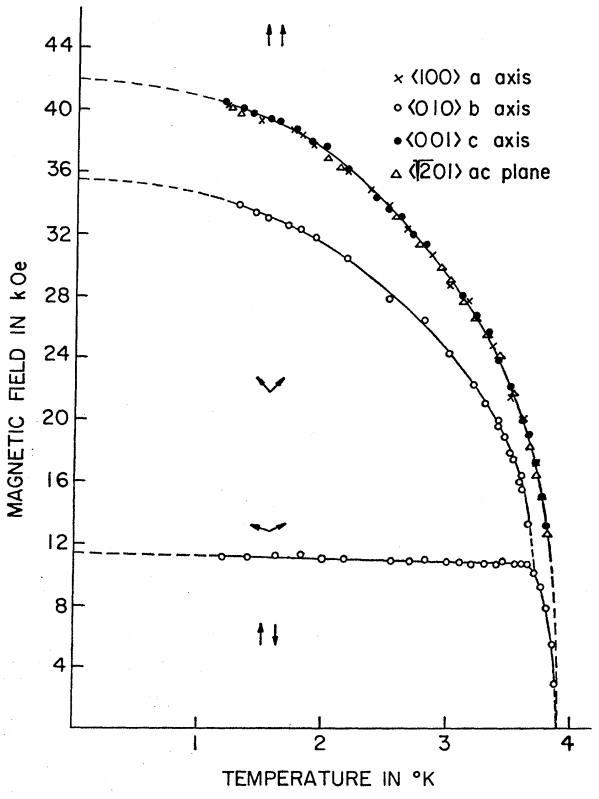

FIG. 6. The magnetic phase diagram of $GdAlO_3$ for various directions of applied magnetic field. The arrows show the relative orientation of the sublattice magnetizations for the field applied along the b axis where the spin flop is observed. For all other directions only the spin-flop-to-paramagnetic phase boundary is given.

done by finding the Brillouin function that gave the smoothest continuation of the experimental curve. This procedure is necessary since the phase boundary does not follow exactly a Brillouin function over the whole temperature range. When the magnetic field is applied along the b axis, H_{c2} is first seen in dM/dH on cooling down to 3.65°K, whereas for other directions it is seen at temperatures as high as 3.80°K. Above 3.80°K the critical field H_{c2} was determined from the temperature dependence of the susceptibility measured for various fields.[14]

The angular variation of H_{c2} was measured in the bc plane and H_{c2} was found to be a minimum for applied fields along the b axis and a maximum along the c axis, as shown in Fig. 7. However, in the ac plane, which is orthogonal to the bc plane, H_{c2} was found to be independent of the direction of the applied field. Such behavior may be explained by an anisotropy field acting along the orthorhombic b axis. The angular variation of H_{c1} was not measured, as the phase transition is seen only as a wide diffuse peak for directions not far from the b axis. It may be noted, however, that the critical field H_{c1} does not show a strong angular dependence in the bc plane.

DISCUSSION

The antiferromagnetic-to-spin-flop critical field H_{c1}, and the angular variation of the spin-flop-to-paramagnetic phase transition in the bc plane may be derived from the free energy of the system in an applied field H. Comparing the results of such a calculation with the experimentally determined critical fields yields the exchange and anisotropy fields at $T=0$°K. The molar free energy of a system of antiferromagnetically coupled spins S with uniaxial anisotropy at $T=0$°K is given by

$$E=\tfrac{1}{2}(g\mu_B SN)[H_{ex}\cos(\theta_1-\theta_2)-\tfrac{1}{2}H_{aL}(\cos^2\theta_1+\cos^2\theta_2)+H_{aK}\cos\theta_1\cos\theta_2-H_y(\sin\theta_1+\sin\theta_2)-H_z(\cos\theta_1+\cos\theta_2)], \quad (1)$$

where θ_1 and θ_2 are the angles the sublattice magnetizations make with the axis of easy magnetization, and H_z and H_y are the components of the applied field parallel and perpendicular to the easy axis of magnetization. The first term is the exchange energy, and the second and third terms are anisotropy energies. Dipolar anisotropy would generally contribute to both these terms, whereas anisotropic exchange would contribute only to H_{aK}, and an axial crystal field would contribute only to H_{aL}. The last two terms are Zeeman energies. The spin-flop-to-paramagnetic critical field is obtained from the instability condition

$$\frac{\partial^2 E}{\partial\theta_1^2}\frac{\partial^2 E}{\partial\theta_2^2}-\left(\frac{\partial^2 E}{\partial\theta_1\partial\theta_2}\right)^2>0, \quad (2)$$

and the equilibrium condition

$$\partial E/\partial\theta_1=\partial E/\partial\theta_2=0 \quad (3)$$

when $\theta_1=\theta_2$. From the above we have

$$H_{c2}\cos\phi=\cos\theta[2H_{ex}+H_{aK}(1+\sin^2\theta)-H_{aL}\cos^2\theta], \quad (4a)$$

$$H_{c2}\sin\phi=\sin\theta[2H_{ex}+H_{aK}\sin^2\theta+H_{aL}\sin^2\theta], \quad (4b)$$

where ϕ is the angle between the applied magnetic field and the b axis.

Equations (4a) and (4b) immediately give the critical field H_{c2} for the applied field parallel and perpendicular to the b axis as

$$H_{c2}(\|)=2H_{ex}+H_{aK}-H_{aL}, \quad (5a)$$

$$H_{c2}(\perp)=2H_{ex}+H_{aK}+H_{aL}. \quad (5b)$$

Equations (5a) and (5b) show that the limits of the angular variation of H_{c2} are determined by H_{aL}.

The lower critical field H_{c1} may also be calculated in terms of the exchange and anisotropy fields. Since the antiferromagnetic-to-spin-flop phase transition is a first-order phase transition, superheating and supercooling are to be expected. However, this is not observed experimentally and, therefore, the observed critical field is identified as the thermodynamical critical field. Setting the energy of the antiferromagnetic phase given by Eq. (1) equal to that of the spin-flop phase, and using the equilibrium condition [Eq. (3)] one obtains for the thermodynamical critical field

$$H_{c1}=[(2H_{ex}+H_{aK}-H_{aL})(H_{aL}+H_{aK})]^{1/2}. \quad (6)$$

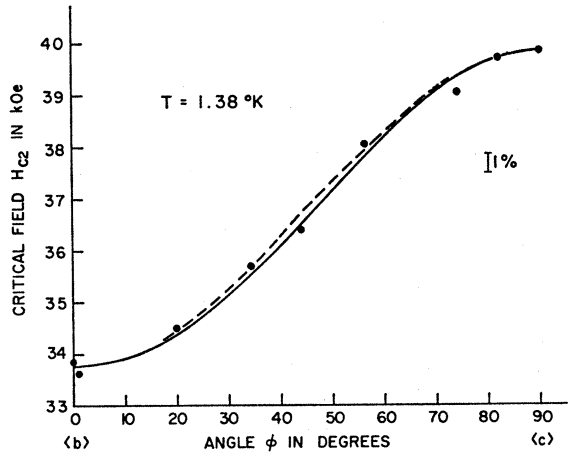

FIG. 7. Angular variation of the spin-flop-to-paramagnetic phase boundary in the bc plane at 1.38°K. The points are the experimental measurements and the solid and broken lines are the theoretical curves derived in the discussion.

[14] W. E. Henry, Phys. Rev. **94**, 1146 (1954).

Combining Eqs. (5) and (6), the molecular fields are expressed in terms of the measured critical fields at $T=0$:

$$H_{ex}=\tfrac{1}{2}[H_{c2}(\perp)-H_{c1}^2/H_{c2}(\|)], \quad (7a)$$

$$H_{aL}=\tfrac{1}{2}[H_{c2}(\perp)-H_{c2}(\|)], \quad (7b)$$

$$H_{aK}=H_{c1}^2/H_{c2}(\|)-\tfrac{1}{2}[H_{c2}(\perp)-H_{c2}(\|)]. \quad (7c)$$

With $H_{c2}(\perp)=42.0$ kOe, $H_{c2}(\|)=35.5$ kOe, and $H_{c1}=11.5$ kOe, one obtains

$$2H_{ex}=38.3\pm0.3 \text{ kOe},$$

$$H_{aL}=3.3\pm0.2 \text{ kOe},$$

$$H_{aK}=0.5\pm0.3 \text{ kOe}.$$

The errors in H_{ex}, H_{aL}, and H_{aK} correspond to an error of $\frac{1}{2}\%$ in the relative measurement of the critical fields. The systematic error in the magnetic field determination is about 2%.

Now that all the parameters of Eqs. (4a) and (4b) have been determined, the angular variation of H_{c2} may be evaluated numerically. The result of such a calculation normalized to the data at 1.38°K gives the solid line shown in Fig. 7, which agrees with the experimental points to better than 1%.

The angular variation of H_{c2} is determined almost entirely by the H_{aL}-type anisotropy field and only slightly affected by H_{aK}. This is also seen in Fig. 7, where the broken curve corresponds to H_{aK} equal to H_{aL}, or 6.5 times larger than the value of H_{aK} used to compute the solid line.

Using the crystal-structure parameters of $DyAlO_3$ Bielen *et al.*[15] have calculated the dipole energies of the possible magnetic structures of $TbAlO_3$. If their values of the molar dipole energies are reduced by the ratio of the squares of the moments of Gd and Tb, one obtains a value of 12.2×10^7 erg for the difference in molar dipole energy for an A_yG_x order with spins parallel and perpendicular to the orthorhombic b axis. This corresponds to a magnetic field of 3.3 kOe acting on each Gd ion, which agrees very well with the value of the anisotropy field determined from the measured critical fields. It appears therefore that the anisotropy in $GdAlO_3$ has its basis in dipole-dipole interactions.

Extrapolation of the spin-flop-to-paramagnetic phase boundary to $T=0$°K defines the critical field H_{c2}, which shows a 20% orientation variation for fields applied parallel and perpendicular to the easy axis of magnetization. However, extrapolation of the same phase boundary to $H=0$ shows only a reduction of 3% in its intercept with the T axis for fields applied parallel to the easy axis with respect to the Néel temperature, which is the intercept measured in fields applied perpendicular to the easy axis. The susceptibility at the Néel temperature also only shows a variation of 2%, which is as large as the experimental error. This is an unexpected result since a molecular-field analysis[16] including dipolar anisotropy predicts a fractional variation in the critical field H_{c2} in the intercept with the T axis and in the susceptibility at the Néel temperature of the same order of magnitude, H_{aL}/H_{ex}. It is thought that this anomaly may be related to the anomalous magnetization data.

From the experimental data the nearest- and next-nearest-neighbor exchange interactions have been evaluated from a molecular-field analysis. Expressions have been derived for Néel temperature, Curie-Weiss Θ, the exchange field H_{ex}, and the susceptibility at the Néel temperature for the three possible types of order of a simple cubic array of Gd ions. Using these four expressions to obtain the two unknowns, consistent results are obtained only for the magnetic order where all the nearest neighbors of any given ion are antiparallel. This is in agreement with the optical determination of the magnetic order by Hawkes and Leask.[17] The values obtained for the nearest-neighbor exchange constant are $J_1/k=-0.07$°K and for the next-nearest-neighbor exchange constant $J_2/k=-0.003$°K.

CONCLUSION

It has been found that $GdAlO_3$ is a uniaxial antiferromagnet at temperatures below 3.89°K. The magnetic phase diagram in the H-T plane has been determined as a function of crystal orientation, and the critical fields determined for $T=0$°K are found to be consistent with an exchange field of 19.15 kOe and a dipolar anisotropy field of 3.3 kOe. A small anisotropic exchange is also found but its existence is not proven.

The magnetization is found to be anomalous in that the full moment of Gd observed in the susceptibility measurements is never observed in the high-field magnetization at low temperatures.

ACKNOWLEDGMENTS

We should like to acknowledge stimulating discussions with J. Feder, E. Pytte, and H. Thomas. We should like to thank H. Keller for designing and constructing the analog function generator used to measure the differential susceptibility. The technical assistance of C. Gerber and H. Neyer is appreciated.

[15] H. J. Bielen, J. Mareschal, and J. Sivardiere, Z. Angew. Phys. **23**, 243 (1967).

[16] H. Thomas (private communications).

[17] J. F. B. Hawkes and M. J. M. Leask, J. Phys. C. **1**, 165 (1968).

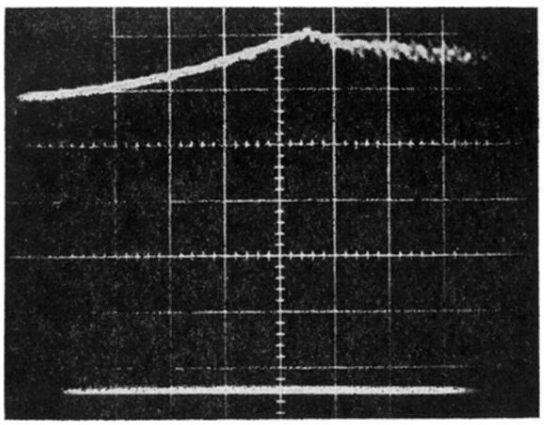

(a) $T=3.80°K$, field scale = 1050 Oe per scale division.

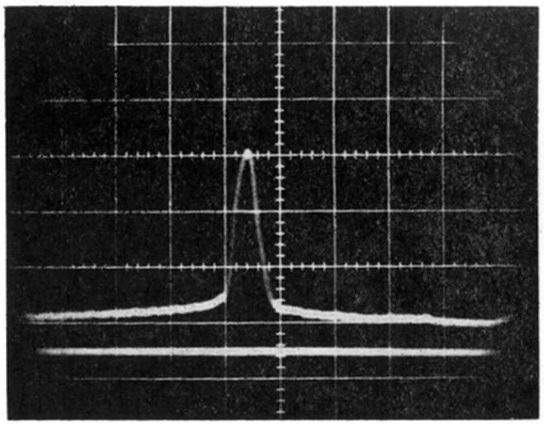

(b) $T=3.50°K$, field scale = 340 Oe per scale division.

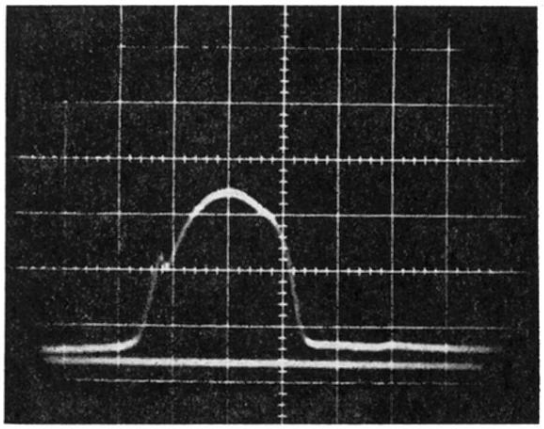

(c) $T=2.50°K$, field scale = 340 Oe per scale division.

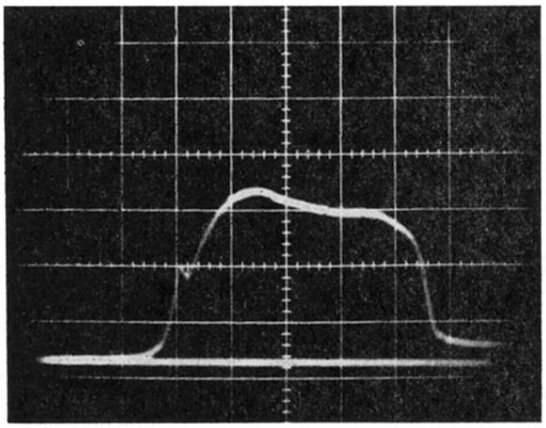

(d) $T=1.25°K$, field scale = 310 Oe per scale division.

FIG. 4. Oscillograms of dM/dH against applied magnetic field showing the growth of the peak due to spin flopping at H_{c1} as a function of temperature. The relative sensitivities (in arbitrary units) of the dM/dH scale are 20:2:1:1 for 3.80, 3.50, 2.50, and 1.25°K, respectively.

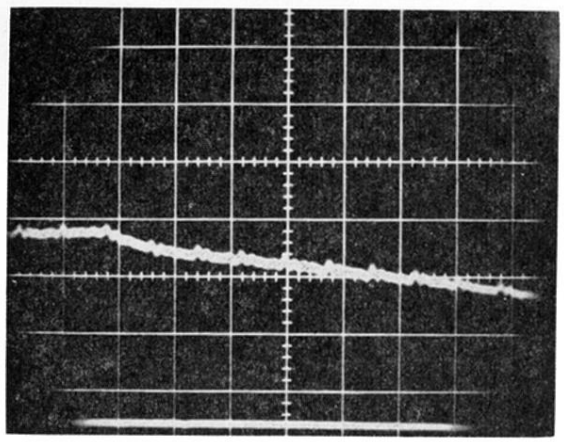

(a) $T=3.50°K$, field scale $=430$ Oe per scale division.

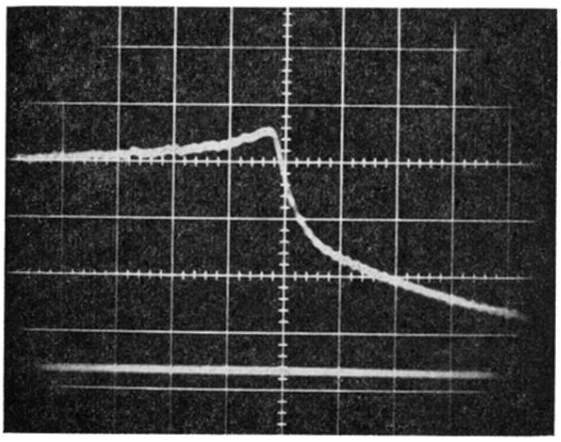

(b) $T=2.50°K$, field scale $=600$ Oe per scale division.

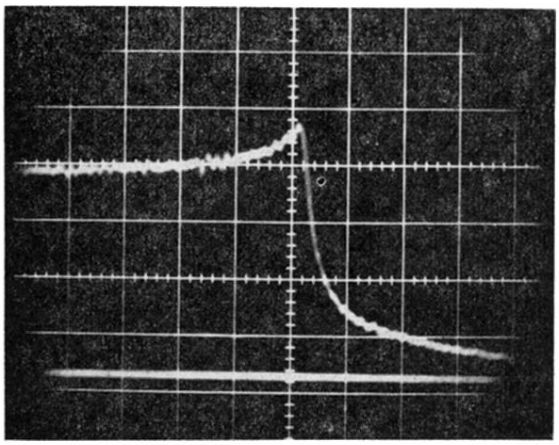

(c) $T=1.25°K$, field scale $=680$ Oe per scale division.

FIG. 5. Oscillograms of dM/dH against applied magnetic field showing the sharp drop in dM/dH on passing through the spin-flop-to-paramagnetic phase boundary at H_{c2}. The sensitivity of dM/dH is the same in all three photographs.